IMECE2006-14426

SUBMICRON THERMAL IMAGING OF HIGH POWER SLAB COUPLED OPTICAL WAVEGUIDE LASER (SCOWL)

Paddy K.L. Chan[1], Amul D. Sathe[1], Kevin P. Pipe[1],
Jason J. Plant[2], Reuel B. Swint[2] and Paul W. Juodawlkis[2]
[1]Department of Mechanical Engineering, University of Michigan, Ann Arbor, MI, USA
[2]Lincoln Laboratory, Massachusetts Institute of Technology, Lexington, MA, USA

ABSTRACT

Nonradiative power dissipation within and near the active region of a high power single mode slab coupled optical waveguide laser is directly measured by CCD-based thermoreflectance, including its variation with device bias. By examining the high spatial resolution temperature profile at the optical output facets, we quantify heat spreading from the source in the active region both downward to the substrate and upward to the metal top contact.

NOMENCLATURE

k_{th}	Thermal conductivity (W/cm-K)
P_{nrr}	Nonradiative recombination power (W)
q	Heat power per unit length (W/cm)
R	Reflectivity
T	Temperature (K)
α	Thermal diffusivity (cm^2/s)
κ	Thermoreflectance coefficient (1/K)
ω	Device bias frequency (1/s)

INTRODUCTION

High power laser diodes have many different kinds of applications such as laser imaging, pumps for solid state lasers, and optical communication. For optical communication, laser light at 1.55 µm is desired because of the low loss in silica-based optical fibers at this particular wavelength. Furthermore, in order to maintain a high quality optical beam over a long distance with high bitrate, single mode fiber is desired. Different laser structures which have high single-mode output power have been developed, such as tapered structures and broad stripe structures. Both types suffer from low efficiency of coupling into single-mode fiber. For broad stripe lasers, the main limitation decreasing the coupling efficiency is the high aspect ratio of the mode. Recently, a new class of semiconductor laser has been developed known as the slab coupled optical waveguide laser (SCOWL).[1] SCOWL is a high power single mode laser diode which can directly butt couple to an optical fiber by taking advantage of its almost circular single mode optical output. While these structures have demonstrated extremely high coupling efficiency, their performance and reliability as lasers as well as optical amplifiers is tied to their operating temperature.[2] High-temperature effects such as decreased efficiency and defect generation are important not only in SCOWL devices but also in high-power lasers generally.

In the present work, we study the temperature distribution on a SCOWL output facet using high resolution CCD-based thermoreflectance. By examining the two dimensional temperature map, we can accurately locate heat source locations and power dissipation mechanisms at the device facet.

Various temperature measurement techniques, such as photoluminescence,[3] Raman scattering,[4] and single-spot thermoreflectance,[5] have been applied to measure the facet temperatures of laser diodes under bias. For photoluminescence and Raman scattering techniques, the temperature resolution is limited by the resolution of the spectrometer which is used to measure the spectrum shift due to device surface temperature change. Single-spot thermoreflectance, in general, has high temperature and time resolution but requires a precise x-y translation stage or scanning optics to generate a 2D map of device temperature.

CCD-based thermoreflectance is a promising temperature measurement approach for microscale electronic and optoelectronic devices due to its high resolution and relatively short experiment time. The working principle of thermoreflectance is to measure the change in reflectivity ΔR of the sample surface due to temperature variation ΔT by the equation

$$\Delta T = \kappa^{-1} \frac{\Delta R}{R} \qquad (1)$$

where κ is known as the thermoreflectance coefficient and depends on both the illuminating wavelength and the sample material. In general, the thermoreflectance coefficent has an order of magnitude $\sim 10^{-3}$-10^{-5} K^{-1} for metals and semiconductors. It can be found for a given sample by calibrating the thermoreflectance signal $\Delta R/R$ with measurements taken over a broad area with a microthermocouple.

FIG. 1. shows the schematic of the experiment setup. A blue LED with $\lambda = 470$nm illuminates the laser through a high-power objective (100x, NA=0.55), using a 45 degree mirror to image the laser facet directly. The reflected image is captured by a 12 bit CCD camera. In order to prevent the thermoreflectance signal from being contaminated by the laser light, a high optical density (OD6) filter is installed on the microscope to filter out the $\lambda=1.55\mu$m SCOWL emission. The device is mounted on a temperature-controlled stage which is maintained at T = 20°C. As shown in FIG. 1, the CCD camera is triggered on each of the rising edges of a 40Hz signal, and the SCOWL is biased by a sine wave at 10Hz; four pictures are taking during each bias period of the SCOWL. The thermoreflectance signal $\Delta R/R$ can be written as a combination of these four images[6]:

$$\frac{\Delta R}{R} = \frac{\pi \sqrt{(I_0 - I_2)^2 + (I_1 - I_3)^2}}{\sqrt{2}(I_0 + I_1 + I_2 + I_3)} \qquad (2)$$

The amplitude of the device temperature variation can then be determined by multiplying the thermoreflectance signal by the reciprocal of the thermoreflectance coefficient. Since the thermoreflectance signal is continuous across the InP and InGaAsP, we can approximate the thermorefectance coefficients of these two materials as nearly the same, using $\kappa = 2.2 \times 10^{-4}$ as calibrated with a microthermocouple. The spatial and temperature resolution of the thermal image are 500nm and 0.5K respectively.

The detailed structure of the 1cm-long SCOWL is shown in FIG. 2(a). The dotted square in FIG. 2(a) corresponds to the region of the 2D temperature map shown in FIG. 2(b). In FIG. 2(b) we can see significant heating near the active region. The dotted line in FIG. 2(b) is the mid-plane cross section slice plotted in FIG. 3.
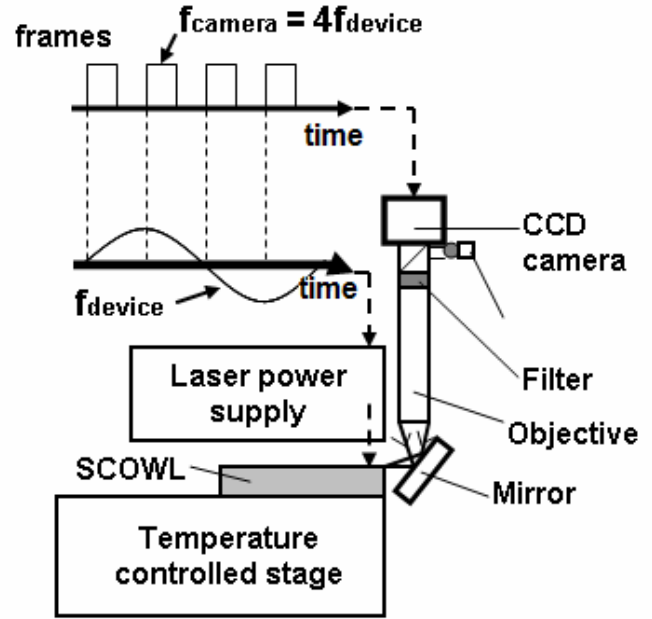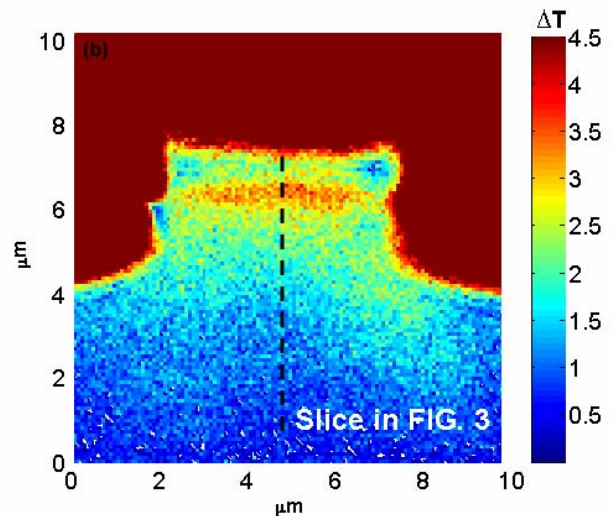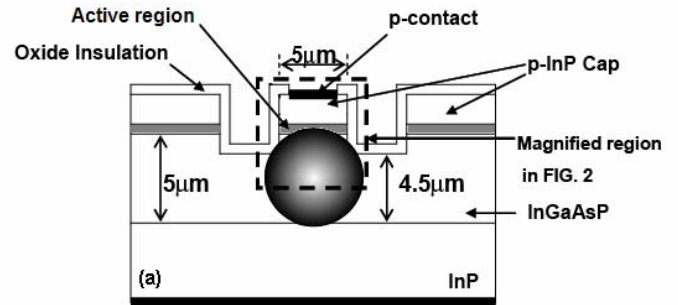

FIG. 1 Schematic of the experimental setup.

FIG. 2 (a) SCOWL structure and (b) 2D temperature map of the SCOWL at I=2.4A.

© 2006 by ASME and MIT Lincoln Laboratory

The temperature profile of a laser diode in a semi-infinite and low bias frequency approximation can be written as[7]

$$T(r) = \frac{q}{k_{th}}\left(\frac{1}{\sqrt{i(\omega/\alpha)}}\right)\frac{K_0\left(\sqrt{i(\omega/\alpha)}r\right)}{K_1\left(\sqrt{i(\omega/\alpha)}r_0\right)} \qquad (3)$$

where q is the heat power per unit length, r_0 is the radial size of the heat source, k_{th} and α are the thermal conductivity and diffusivity of the laser structure, ω is the laser bias frequency, and K_0 and K_1 is the zero and first order of second kind modified Bessel function. The normalized experimental result and analytical solution of the device mid-plane cross section temperature at I=1.2A are plotted in FIG. 3. By normalizing and fitting the analytical temperature profile with the experimental temperature profile at low bias level, we obtain the thermal diffusivity of the laser as 0.628 cm^2/s, which is similar to prior measurements of InGaAsP-based lasers.[8]

In order to determine the origins of the heat source mechanisms measured in the device, we lower the bias frequency of the device to 5Hz and leave the camera taking pictures at 40Hz. The second harmonic temperature variation due to Joule heating (I^2R) is expected to occur at 2×5Hz =10Hz. The first harmonic thermoreflectance signal (which contains both nonradiative recombination and Joule heating components) is much stronger than the second harmonic signal as shown in FIG. 4., suggesting that Joule heating does not play a major role in the heating shown in the highly magnified 2D temperature map.
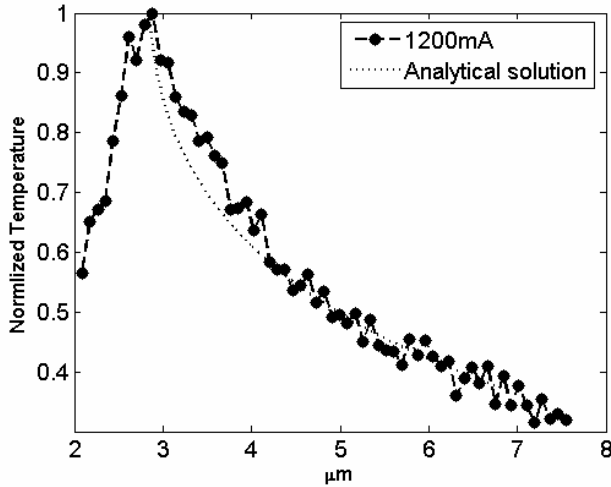

FIG. 3 Experimental and theoretical solution of the normalized temperature profile at I=1.2A. The analytical solution is obtained using $\alpha_{InGaAsP}$ = 6.28 × 10^{-5} m^2/s.
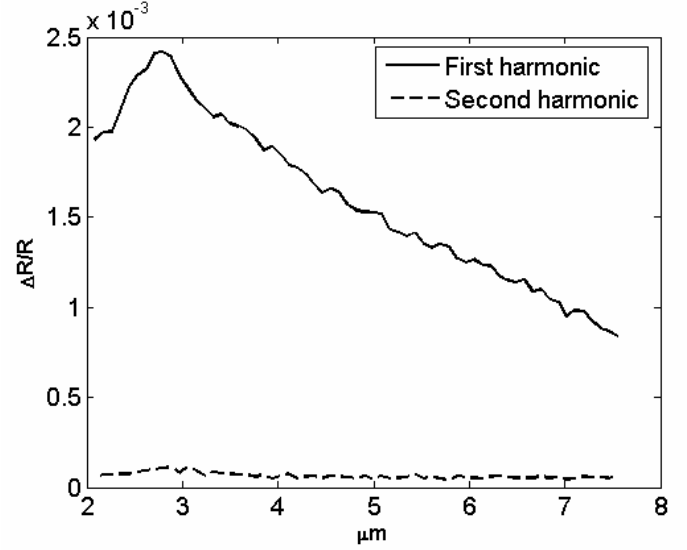

FIG. 4 First and second harmonics of the thermoreflectance signal at I=6A. The second harmonic thermoreflectance signal is much weaker than the first harmonic, suggesting that Joule heating is negligible in the device.

Auger recombination in the InGaAsP active region and carrier leakage from the active region have been considered to be the main efficiency loss mechanisms in InGaAsP laser diodes.[9,10] In addition, optical absorption as well as Shockley-Reed-Hall and surface recombination mechanisms can contribute to efficiency loss. The temperature variations at the active region and the p-InP cap for different device currents are plotted in FIG. 5(a). In order to quantitatively verify the power dissipated as nonradiative recombination (P_{nrr}) at the active region, a 1-dimensional thermal circuit is used to determine the upward and downward heat flows. In the thermal circuit shown in FIG. 5(b), Z_{up} and Z_{down} are the upward and downward thermal impedances respectively and are given by[11]

$$Z_{up} = \frac{L}{k_{p-InP}A}$$

and

$$Z_{down} = \frac{\ln(4h/w)}{\pi kl} \qquad (4)$$

where h, w, and l are the thickness, width, and length of the device, L is the height, and A is the cross-sectional area of the p-InP. FIG. 5(c) shows the calculated P_{nrr} at different currents. It can be observed that the nonradiative power dissipation increases with increasing input current. From FIG. 3(a) we can see that there is a significant temperature gradient between the active region and the p-InP cap layer. This suggests that
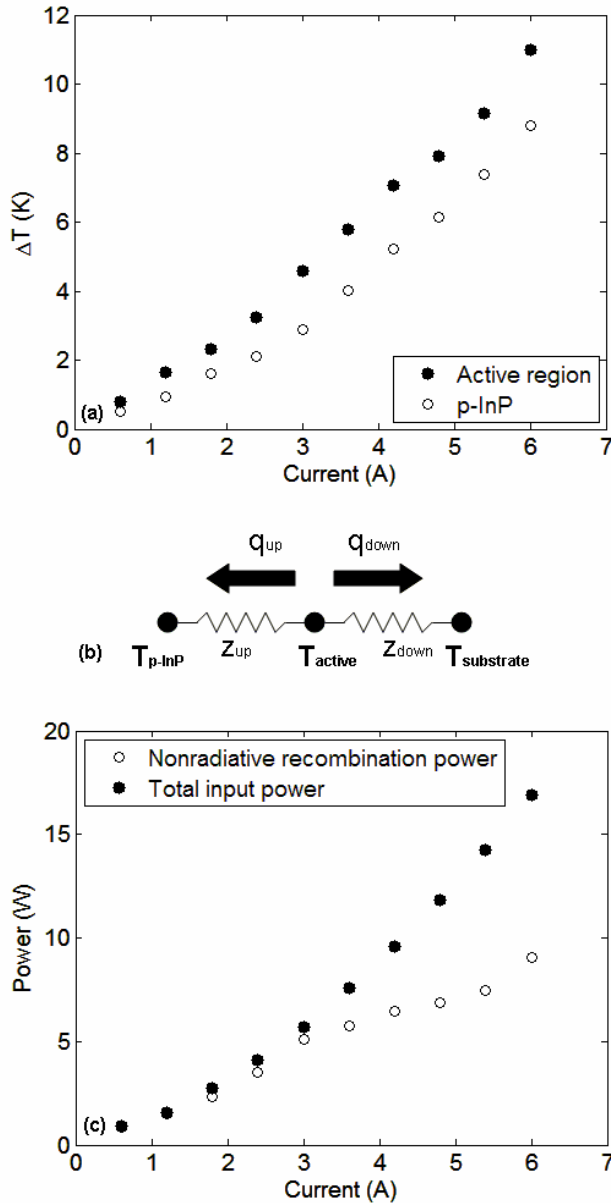
FIG. 5 (a) Temperature variation at the active region and the p-InP cap at different current levels. (b) Schematic of the thermal circuit; z_{th} = 0.59 K/W and z_{down} = 2.1 K/W are the upward and downward thermal impedances. (c) Nonradiative recombination power and total input power plotted as a function of current.

only considering the heat flux downward from the active region will underestimate the nonradiative recombination power; for accurate estimation of the nonradaitive heating within the active region of the device, it is necessary to also consider the heat flux flowing upward from the active region into the p-InP and top metal contact. It also implies that the surface temperature of the top metal contact is actually lower than the true active region temperature by a significant amount (>20%), especially at high bias levels. This is important because the laser active region temperature (which sets the performance

characteristics of the device) has in the past been approximated by top contact measurements.[12]

In conclusion, we demonstrate that by using a high resolution CCD-based 2D thermoreflectance method we can measure nonradiative recombination power within a laser directly by determining the temperatures of the p-InP cap, active region, and substrate. We find that approximating the top metal contact temperature as the active region temperature can cause errors of more than 20%; a high resolution temperature map is needed to obtain this value accurately.

REFERENCES

[1] Plant, J.J., Juodawlkis, P.W.; Huang, R.K., Donnelly, J.P., Missaggia, L.J. and Ray, K.G., 2005, "1.5-µm InGaAsP-InP slab-coupled optical waveguide lasers", IEEE Photonics Technology Letters, 17(4), 735-737

[2] Juodawlkis, P.W., Plant, J.J., Huang, R.K., Missaggia, L.J. and Donnelly, J.P., 2005, "High-power 1.5-µm InGaAsP-InP slab-coupled optical waveguide amplifier", IEEE Photonics Technology Letters, 17(2), 279-281

[3] Spagnolo, V., Troccoli, M., Scamarcio, G., Gmachl, C., Capasso, F., Tredicucci, A., Sergent, A.M.; Hutchinson, A.L., Sivco, D.L. and Cho, A.Y., 2001, "Temperature profile of GaInAs/AlInAs/InP quantum cascade-laser facets measured by microprobe photoluminescence", Applied Physics Letters, 78 (15), p 2095-2097

[4] Herrmann, F.U., Beeck, S., Abstreiter, G.., Hanke, C., Hoyler, C. and Korte, L., 1991, "Reduction of mirror temperature in GaAs/AlGaAs quantum well laser diodes with segmented contacts" Applied Physics Letters, 58 (10), 1007—1009

[5] Lewis, D., Dihaire,S., Phan, T.,, Quintard, V., Horrnung, V. and Claeys., W., 1998, "Modeling and experimental study of heat deposition and transport in a semiconductor laser diode," Microelectronics Journal, 29, 171-179.

[6] Grauby, S., Forget, B.C., Hole, S. and Fournier, D., 1999, "High resolution photothermal imaging of high frequency phenomena using a visible charge coupled device camera associated with a multichannel lock-in scheme", Review of Scientific Instruments, 70 (9), 3603-3608

[7] Carlslaw, H. S. and Jaeger, J. C., 1993, Conduction of Heat in Solids, Clarendon Press, Oxford

[8] Zhu, C., Zhang, Y.G., Li, A.Z. and Zheng, Y.L., 2005, "Comparison of thermal characteristics of antimonide and phosphide MQW lasers", Semiconductor Science and Technology, 20 (6), 563-567

[9] Sugimura, A., 1981, "Band-to-band Auger recombination effect on InGaAsP laser threshold", IEEE Journal of Quantum Electronics, 17 (5), 627-635

[10] Piprek, J., Abraham, P. and Bowers, J.E., 2000, "Self-consistent analysis of high-temperature effects on strained-layer multiquantum-well InGaAsP-InP lasers', IEEE Journal of Quantum Electronics, 36 (3), 2000, 366-374

[11] Coldren, L. A. and Corzine, S. W., 1995, Diode Lasers and Photonic Integrated Circuits, Wiley

[12] Pipe, K.P. and Ram, R.J., 2003, "Comprehensive heat exchange model for a semiconductor laser diode", IEEE Photonics Technology Letters 15 (4), 504-506